Performance Enhancement of Anisotropic Scattering Treatment in MOC Calculation by Angular Flux Storage

Min Ryu and Han Gyu Joo *
Seoul National University, 1 Gwanak-ro Gwanak-gu, Seoul, 151-744, Korea
**Corresponding author: joohan@snu.ac.kr*

1. Introduction

In order to incorporate anisotropic scattering in the Method of Characteristics (MOC) transport calculations, explicit anisotropy treatment schemes that employ angular flux moments associated with spherical harmonics were implemented in numerous direct whole calculation codes such as nTRACER[1] and its effective has been examined with various benchmark problems[2,3]. In this method, region averaged anglur flux moments such as scalar flux and current are calculated during the ray tracing calculations. In this on-the-fly moment calculation, proper angle dependent weight terms are necessary that are derived using spherical harmonics[2]. Although higher order expansions would give more accurate solutions, it turned out that normally second order expansion could provide quite accurate results in PWR analyses. In two dimensional (2D) MOC calculations, additional five angular flux moment terms are required for the second order expansion and the calculation of these terms can induce significant computational overhead during the ray tracing calculation.

In nTRACER[1], the default ray tracing module was established with the isotropic scattering treatment and it was optimized for parallel calculation using OpenMP. In this calculation module, so called the Flux Moment Storage Scheme (FMSS) has been used with an efficient two-step calculations which will be presented in the following sessions. Since this scheme requires quite significant computing time for higher order scattering treatments, the Angular Flux Storage Scheme (AFSS) is tried in this work that requires three step calculations. The details of the implementation of the AFSS in nTRACER and the performance examination results are presented in this paper.

2. nTRACER Ray Tracing Scheme

Consider a typical radial geometry of a reactor shown in Fig. 1 that consists of properly discretized flat source regions (FSRs). Then the segment averaged angular flux is represented as:

$$\bar{\varphi}_{l,m,k}^{g,n} = \frac{1}{s_{l,k}^n}\int_0^{s_{l,k}^n} \varphi_{l,m,k}^{g,n}(s)ds = \frac{\varphi_{l,m,k}^{in,g,n} - \varphi_{l,m,k}^{out,g,n}}{\Sigma_t^{g,n} s_{l,k}^n / \sin\theta_m} + \frac{q_{l,m}^{g,n}}{\Sigma_t^{g,n}}. \quad (1)$$

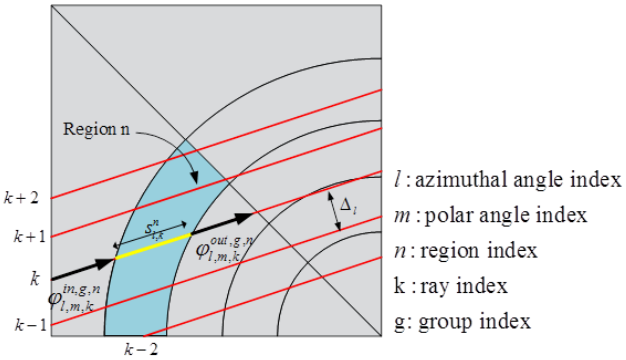

Fig. 1. Typical radial geometry of a region and MOC ray structures

With above equation, the region averaged angular flux can be easily derived as follows:

$$\bar{\varphi}_{l,m}^{g,n} = \frac{\sum_{k\in n}\bar{\varphi}_{l,m,k}^{g,n} s_{l,k}^n \Delta_l}{\sum_{k\in n} s_{l,k}^n \Delta_l} = \frac{\sin\theta_m}{\Sigma_t^{g,n}} \frac{\sum_{k\in n}\left(\varphi_{l,m,k}^{in,g,n} - \varphi_{l,m,k}^{out,g,n}\right)\Delta_l}{\sum_{k\in n} s_{l,k}^n \Delta_l} + \frac{q_{l,m}^{g,n}}{\Sigma_t^{g,n}}. \quad (2)$$

The region averaged high order angular flux moment is then obtained as follows:

$$\begin{aligned}\bar{\phi}_{L,M}^{g,n} &= \sum_{l,\mathrm{m}} w_{l,m}\bar{\varphi}_{l,m}^{g,n} Y_{L,M}^*(\mu_m,\alpha_l) \\ &= \sum_{l,m} w_{l,m}\left(\frac{\sin\theta_m}{\Sigma_t^{g,n}} \frac{\sum_{k\in n}\left(\varphi_{l,m,k}^{in,g,n} - \varphi_{l,m,k}^{out,g,n}\right)\Delta_l}{\sum_{k\in n} s_{l,k}^n \Delta_l} + \frac{q_{l,m}^{g,n}}{\Sigma_t^{g,n}}\right) Y_{L,M}^*(\mu_m,\alpha_l)\end{aligned} \quad (3)$$

where the spherical harmonics function is given as:

$$Y_{L,M}(\mu_m,\alpha_l) = \sqrt{\frac{(L-M)!}{(L+M)!}} P_L^M(\mu_m)\exp(iM\alpha_l), \mu_m = \cos\theta_m. \quad (4)$$

Then source term in Eq. (2) can be represented by the following Legendre expansion:

$$\begin{aligned} q_{l,\mathrm{m}}^{g,n} &= q^{g,n,f} + \sum_L \sum_{M=-L}^{L} q_{l,m}^{g,n,\mathrm{s,L,M}} \\ &= \frac{1}{4\pi}\chi_g\psi + \sum_{g'}\sum_L \sum_{M=-L}^{L} \frac{2L+1}{4\pi}\Sigma_s^{g'g,n,(L)}\bar{\phi}_{L,M}^{g,n} Y_{L,M}(\mu_m,\alpha_l) \end{aligned}. \quad (5)$$

Using the following orthogonality of the spherical harmonics shown:

$$\int_{4\pi} w_{l,m} Y_{L,M}(\theta_m,\alpha_l) Y_{L',M'}^*(\theta_m,\alpha_l)\sin\theta_m d\Omega = \frac{4\pi}{2L+1}\delta_{LL'}\delta_{MM'} \quad (6)$$

the region averaged high order angular flux moment is simplified as follows:

$$\bar{\phi}_{L,M}^{g,n} = \sum_{l,m} w_{l,m} \frac{\sin\theta_m}{\Sigma_t^{g,n}} \frac{\sum_{k\in n}\left(\varphi_{l,m,k}^{in,g,n} - \varphi_{l,m,k}^{out,g,n}\right)\Delta_l}{\sum_{k\in n} s_{l,k}^n \Delta_l} Y_{L,M}^*(\mu_m,\alpha_l) + \delta_{0L}\frac{\chi_g \psi}{\Sigma_t^{g,n}} + \frac{1}{\Sigma_t^{g,n}}\sum_{g'}\Sigma_s^{g'g,n,(L)}\bar{\phi}_{L,M}^{g,n} \quad (7)$$

In order to satisfy the neutron balance equation, so called volume correction should be considered. After volume correction, Eq. (7) can be re written as follows and Table 2 shows the number of required flux moments for the expansion upto the 3rd order.

$$\bar{\phi}_{L,M}^{g,n} = \frac{1}{\Sigma_t^{g,n}V^n}\sum_{l,m} w_{l,m}\sin\theta_m \sum_{k\in n}\left(\varphi_{l,m,k}^{in,g,n} - \varphi_{l,m,k}^{out,g,n}\right)\Delta_l Y_{L,M}^*(\mu_m,\alpha_l) + \frac{Q^{g,n,L}}{\Sigma_t^{g,n}} \quad (8)$$

Table 1. Number of flux moments for n-th order expansion

Scattering Expansion Order	1D	**2D**	3D
0th	1	**1**	1
1st	2	**3**	4
2nd	3	**6**	9
3rd	4	**10**	16

In the following two subsections, the methods for obtaining the angular moments of sources are detailed.

2.1 Flux Moment Storage Scheme

In the previous ray tracing module which is for the MOC calculation with transport corrected cross sections and the isotropic scattering treatment, an efficient calculation scheme was applied with the FMSS that accumulates only the angle dependent terms with one tiny ray segment, not including the term due to the source in Eq. (8):

$$\hat{\phi}_{0,0}^{g,n} = \sum_{l,m} w_{l,m}\sin\theta_m \sum_{k\in n}\left(\varphi_{l,m,k}^{in,g,n} - \varphi_{l,m,k}^{out,g,n}\right)\Delta_l Y_{0,0}^*(\mu_m,\alpha_l)\,. \quad (9)$$

Since the above term is not angle dependent, the memory requirement for saving $\hat{\phi}_{0,0}^{g,n}$ is not an important concern. After all ray tracing calculations, the region averaged scalar flux is obtained as:

$$\bar{\phi}_{0,0}^{g,n} = \frac{\hat{\phi}_{0,0}^{g,n}}{\Sigma_t^{g,n}V^n} + \frac{Q^{g,n,0}}{\Sigma_t^{g,n}}\,. \quad (10)$$

This is the two-step procedure to obtain the region average scalar flux.

For high order expansions, additional memories for saving the high order flux moment terms $\bar{\phi}_{L,M}^{g,n}$ defined by:

$$\hat{\phi}_{L,M}^{g,n} = \sum_{l,m} w_{l,m}\sin\theta_m \sum_{k\in n}\left(\varphi_{l,m,k}^{in,g,n} - \varphi_{l,m,k}^{out,g,n}\right)\Delta_l Y_{L,M}^*(\mu_m,\alpha_l) \quad (11)$$

are required during the ray tracing with the FMSS scheme. After accumulating the above term, the same procedure as the scalar flux is performed to determine the region average angular flux moments:

$$\bar{\phi}_{L,M}^{g,n} = \frac{\hat{\phi}_{L,M}^{g,n}}{\Sigma_t^{g,n}V^n} + \frac{Q^{g,n,L}}{\Sigma_t^{g,n}}\,. \quad (12)$$

However, this two-step procedure with the FMSS induces an increase in the computing time because the accumulation of the $\hat{\phi}_{L,M}^{g,n}$ terms for each ray segment by multiplying different angle dependent factors increases the number of multiplication operations and this is the major drawback of the FMSS for high order cases.

2.2 Angular Flux Storage Scheme

To mitigate the drawback of the FMSS, the AFSS was implemented in nTRACER following a three step procedure that increases the memory requirement. The concept of the AFSS is quite simple in that only the differences of incoming and outgoing angular flux are accumulated as shown in below:

$$\hat{\varphi}_{l,m}^{g,n} = \sum_{k\in n}\left(\varphi_{l,m,k}^{in,g} - \varphi_{l,m,k}^{out,g}\right) \quad (13)$$

instead of accumulating the angle dependent term given by Eqs. (9) or (11). The above term is, however, angle dependent, additional memories are required for saving this. The additional amount of the memory will be discussed in the following sessions. On the contrary, since $\hat{\varphi}_{l,m}^{g,n}$ is independent of $Y_{L,M}^*(\mu_m,\alpha_l)$, only $\hat{\varphi}_{l,m}^{g,n}$ term is necessary during the ray tracing calculation regardless of the order of expansion. After all ray tracing calculations, $\hat{\phi}_{L,M}^{g,n}$ in Eq. (11) can be calculated as follows:

$$\hat{\phi}_{L,M}^{g,n} = \sum_{l,m} w_{l,m}\sin\theta_m \Delta_l Y_{L,M}^*(\mu_m,\alpha_l)\hat{\varphi}_{l,m}^{g,n}\,. \quad (14)$$

Then, by using Eq. (12), the region averaged flux moments can be calculated for the update of scattering source in the next MOC iteration. This three-step procedure can reduce the number of multiplication operations significantly during the ray tracing calculation.

3. Examination of Effectiveness

In order to examine the effectiveness of the AFSS, the upgraded version of nTRACER was applied to selected VERA benchmark [4] problems: A) Problem 2A, 2D assembly problem, B) Problem 4A-2D 3x3 mini-core problem and C) Problem 5A-2D quarter core

problem. The geometrical specifications of selected problems are shown in Fig. 2 through Fig. 3.

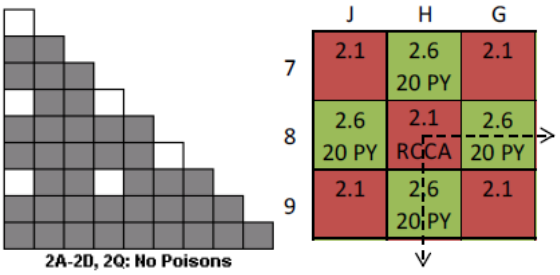

Fig. 2. VERA problem 2A and 4A-2D configuration [4]

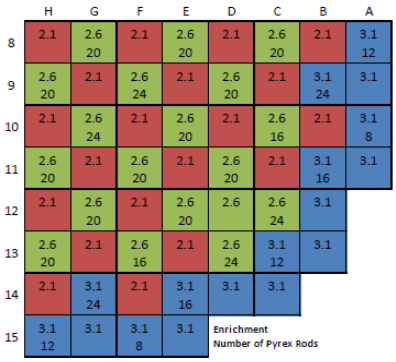

Fig. 3. VERA problem 5A-2D configuration [4]

In the nTRACER calculations for the above problems, the ray spacing used was .05 cm and the numbers of azimuthal angles and optimum polar angles per octant of the solid angle sphere are 12 and 4 for all the cases. Table 2 below shows the basic ray counts of the selected benchmark problems along with the number of flat source regions. It turned out that the AFSS needs 3 GByte of additional memory compared to the FMSS to store $\hat{\varphi}_{l,\mathrm{m}}^{g,n}$ for the core problem (5A-2D). This amount of memory increase can be readily accommodated by modern LINUX cluster machines.

Table 2. Ray structures of selected benchmark problems

Description	2A	4A-2D	5A-2D
# of FSRs	30,016	58,092	1,503,450
# of Rotational Rays	36	54	55,930
# of Segments	3,369,976	6,564,638	167,660,689

To compare the performances of the two schemes, the averaged computing times spent for four independent multi-group MOC sweeps were used. The test calculations were performed on a LINUX cluster mounting 2.67 GHz Intel Xeon 5650 processors. Figs. 4 through 6 show the results of computing time ratio between the compared cases and the fastest case. In the case of P_0 MOC calculations, the FMSS always gives better performance than the AFSS since $\hat{\varphi}_{l,\mathrm{m}}^{g,n}$ terms are stored in multi-dimensional arrays and this massive storage induces nontrivial increase in the memory access times. However once $\hat{\varphi}_{l,\mathrm{m}}^{g,n}$ are calculated and stored, calculating $\hat{\phi}_{\mathrm{L,M}}^{g,n}$ terms is much cheaper than FMSS because of much less multiplication operations for each ray segment. In the case of P_2 MOC, about 50% computing time improvement can be obtained for the all test cases. It is noted that AFSS causes much more moderate increase in the computing time with the number of the flux moment order. Therefore, the AFSS is much more effective with higher scattering order.

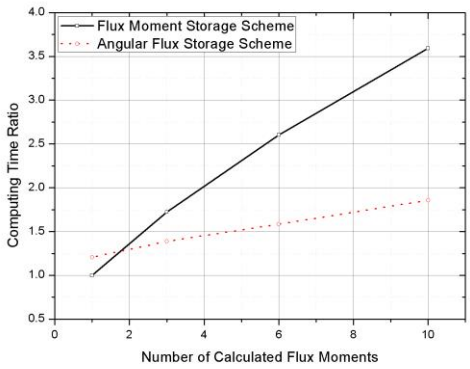

Fig. 4. Computing time ratio results for VERA problem 2A – 2D assembly problem

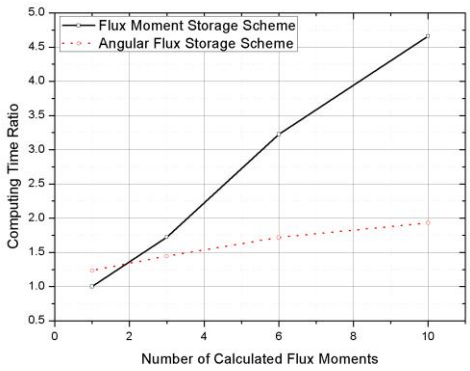

Fig. 5. Computing time ratio results for VERA problem 4A-2D 3x3 mini-core problem

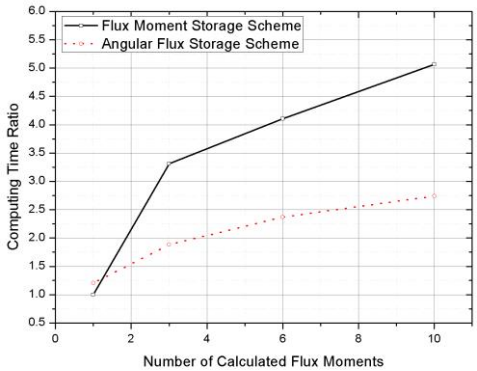

Fig. 6. Computing time ratio results for VERA problem 5A-2D quarter core problem

4. Conclusions

The angular flux storage scheme (AFSS) for the MOC calculations with the scattering anisotropic treatment with spherical harmonic expansion was implemented successfully in the nTRACER direct whole core calculation code. It was noted that although the AFSS shows slightly worse performance for the case of P_0 MOC calculations, it renders about 50% computing time saving in the case of P_2 MOC calculations. Furthermore, the computing time with AFSS shows weak dependency on the order of scattering. This advantage would be every effective in fast reactor applications of the MOC transport solver since at least fifth order scattering is recommended to properly deal with anisotropy scattering in fast reactors. Although the AFSS requires additional memories for the angle dependent terms during the ray tracing calculation, it turned out to that the increase of about 3 GB for the quarter core problem of a realistic reactor is manageable on an affordable LINUX cluster. Thus the AFSS is recommended in the future applications of MOC since the much bigger memories will be readily available in future machines.

Acknowledgements

The authors thank Dr. Richard Sanchez of CEA for informing the basic concept of AFSS. This work was supported by National Research Foundation of Korea (NRF) Grant No. 2014M2A8A2074094.

REFERENCES

[1] Y. S. Jung, C. B. Shim, and H. G. Joo, Practical Numerical Reactor Employing Direct Whole Core Neutron Transport and Subchannel thermal/hydraulic Solvers, Annals of Nuclear Energy Vol.62, p.357-374, 2013.
[2] M. Ryu, Y. S. Jung, C. H. Lim, and H. G. Joo, Incorporation of Anisotropic Scattering in nTRACER, Transactions of Korean Nuclear Society Autumn Meeting, Oct. 30-31, 2014, Pyeongchang, Korea.
[3] S. G. Stimpson, An Azimuthal, Fourier Moment-Based Axial SN solver for the 2D/1D Scheme, Ph.D Thesis, University of Michigan, 2015.
[4] A. T. Godfrey, Vera Core Physics Benchmark Progression Problem Specifications, Revision 3, CASL-U2012-0131-003, CASL, March 31, 2014.